AIP | Journal of Mathematical Physics

Numerical solution of the time dependent Ginzburg-Landau equations for mixed (d + s)-wave superconductors

W. C. Gonçalves, E. Sardella, V. F. Becerra, M. V. Milošević, and F. M. Peeters

Citation: Journal of Mathematical Physics **55**, 041501 (2014); doi: 10.1063/1.4870874
View online: http://dx.doi.org/10.1063/1.4870874
View Table of Contents: http://scitation.aip.org/content/aip/journal/jmp/55/4?ver=pdfcov
Published by the AIP Publishing

Articles you may be interested in

Time dependent Ginzburg-Landau equation for sheared granular flow
AIP Conf. Proc. **1501**, 1001 (2012); 10.1063/1.4769651

Eilenberger and Ginzburg-Landau models of the vortex core in high κ-superconductors
J. Appl. Phys. **110**, 033911 (2011); 10.1063/1.3610502

Existence of the weak solution of coupled time-dependent Ginzburg–Landau equations
J. Math. Phys. **51**, 033507 (2010); 10.1063/1.3293968

Critical State Simulation of the Superconducting Layered Structures Based on Numerical Solution of the GinzburgLandau Equations
AIP Conf. Proc. **850**, 817 (2006); 10.1063/1.2354955

Classical solutions to the time-dependent Ginzburg–Landau equations for a bounded superconducting body in a vacuum
J. Math. Phys. **46**, 095104 (2005); 10.1063/1.2012107

This article is copyrighted as indicated in the article. Reuse of AIP content is subject to the terms at: http://scitation.aip.org/termsconditions. Downloaded to IP: 186.217.234.103 On: Fri, 10 Oct 2014 16:39:20

JOURNAL OF MATHEMATICAL PHYSICS **55**, 041501 (2014)

Numerical solution of the time dependent Ginzburg-Landau equations for mixed ($d + s$)-wave superconductors

W. C. Gonçalves,[1] E. Sardella,[1,2] V. F. Becerra,[3] M. V. Milošević,[3,4] and F. M. Peeters[3,4]
[1]*Departamento de Física, Faculdade de Ciências, Univ Estadual Paulista - UNESP, Caixa Postal 473, CEP 17033-360, Bauru, SP, Brazil*
[2]*UNESP-Universidade Estadual Paulista, IPMet-Instituto de Pesquisas Meteorológicas, CEP 17048-699 Bauru, SP, Brazil*
[3]*Departement Fysica, Universiteit Antwerpen, Groenenborgerlaan 171, B-2020 Antwerpen, Belgium*
[4]*Departamento de Física, Universidade Federal do Ceará, 60455-900 Fortaleza, Ceará, Brazil*

(Received 30 July 2013; accepted 28 March 2014; published online 15 April 2014)

The time-dependent Ginzburg-Landau formalism for ($d + s$)-wave superconductors and their representation using auxiliary fields is investigated. By using the link variable method, we then develop suitable discretization of these equations. Numerical simulations are carried out for a mesoscopic superconductor in a homogeneous perpendicular magnetic field which revealed peculiar vortex states. © *2014 AIP Publishing LLC*. [http://dx.doi.org/10.1063/1.4870874]

I. GINZBURG-LANDAU MODEL FOR *d*-WAVE SUPERCONDUCTORS

It is well known that the physical properties of conventional superconducting materials can be conveniently described by the time dependent Ginzburg-Landau (TDGL) equations, strictly valid only at temperatures close to T_c, but in practice giving very good phenomenological description even at much lower temperature.[1] The unknown functions of these equations are the scalar *complex order parameter* ψ, and the *vector potential* $\mathbf{A}$. The absolute order parameter squared $|\psi|^2$ then represents the *Cooper-pair density*, and the *magnetic induction* $\mathbf{B}$ is found via the equation $\mathbf{B} = \nabla \times \mathbf{A}$. However, conventional superconductors possess s-wave pairing symmetry. For the high critical temperature superconductors, the scalar order parameter is replaced by a multicomponent one with d-wave pairing symmetry. In fact, unconventional superconducting materials often exhibit a mixed ($d + s$)-wave symmetry with two order parameters (ψ_d, ψ_s). In such a case, the TDGL equations are written as

$$\frac{\hbar^2}{2m_d^* D}\left(\frac{\partial}{\partial t} + \frac{ie^*}{\hbar}\varphi\right)\psi_d = -\frac{\delta \mathscr{L}}{\delta \bar{\psi}_d}, \tag{1}$$

$$\frac{\hbar^2}{2m_s^* D}\left(\frac{\partial}{\partial t} + \frac{ie^*}{\hbar}\varphi\right)\psi_s = -\frac{\delta \mathscr{L}}{\delta \bar{\psi}_s}, \tag{2}$$

$$\frac{\sigma}{c}\left(\frac{1}{c}\frac{\partial \mathbf{A}}{\partial t} + \nabla\varphi\right) = -\frac{\delta \mathscr{L}}{\delta \mathbf{A}} - \frac{1}{4\pi}\nabla \times \mathbf{B}, \tag{3}$$

 © 2014 AIP Publishing LLC

This article is copyrighted as indicated in the article. Reuse of AIP content is subject to the terms at: http://scitation.aip.org/termsconditions. Downloaded to IP: 186.217.234.103 On: Fri, 10 Oct 2014 16:39:20

where $\mathscr{L}$ is the Helmholtz *free-energy density functional* which is expressed in terms of two components of the order parameter and the vector potential as

$$\begin{aligned}\mathscr{L} = &-\alpha_s|\psi_s|^2 - \alpha_d|\psi_d|^2 + \frac{\beta_1}{2}|\psi_s|^4 + \frac{\beta_2}{2}|\psi_d|^4 + \frac{\beta_3}{2}|\psi_s|^2|\psi_d|^2 \\ &+\frac{\beta_4}{2}\left(\bar{\psi}_s^2\psi_d^2 + \bar{\psi}_d^2\psi_s^2\right) + \frac{1}{2m_s^*}|\mathbf{\Pi}\psi_s|^2 + \frac{1}{2m_d^*}|\mathbf{\Pi}\psi_d|^2 \\ &+\frac{1}{2m_v^*}\left(\bar{\Pi}_y\bar{\psi}_s\Pi_y\psi_d + \bar{\Pi}_y\bar{\psi}_d\Pi_y\psi_s - \bar{\Pi}_x\bar{\psi}_s\Pi_x\psi_d - \bar{\Pi}_x\bar{\psi}_d\Pi_x\psi_s\right). \end{aligned} \tag{4}$$

Here, the overbar denotes the complex conjugation, and the *covariant derivative* operator is $\mathbf{\Pi} = (-i\hbar\nabla - \frac{e^*}{c}\mathbf{A})$. φ is the scalar electric potential; m_i^* (for $i = d, s, v$) are the effective masses; m_d^* and m_d^* are the effective masses in the d and s band, respectively; m_v^* represents the coupling between the gradient terms, in different bands, in the free-energy density; e^* is the effective charge of the Cooper-pair; D is the phenomenological diffusion coefficient; and σ is the electrical conductivity; β_i ($i = 1, 2, 3, 4$) are positive phenomenological constants and do not depend on temperature; α_d and α_s are also two phenomenological constants. The values of these phenomenological constants have been found from microscopic considerations in Ref. 2 (see also Ref. 3), but we prefer to develop a method of solution of the TDGL equations in a more general scenario. In the latter references, it was shown that $\alpha_d = \alpha_{d0}(T/T_c - 1)$, where α_{d0} is a negative constant and T_c is the critical temperature; α_s is a temperature independent constant, and is negative.[4]

The TDGL equation for a single order parameter was first proposed by Schmid[5] and derived from the microscopic BCS theory by Gor'kov and Eliashberg.[6] The extension of this equation for multicomponent order parameter system with mixed ($d + s$)-wave symmetry was proposed by Du.[7] The free-energy of this system has been proposed by several authors (see, for instance, Refs. 8 and 9) and derived microscopically in Ref. 2.

In order to solve Eqs. (1)–(3), we will follow the same approach used in the pioneering works of Refs. 10 and 11. A more comprehensible solution of these equations have been presented in Ref. 12 for the two-dimensional case and in Ref. 13 for the case of charged boundaries. The generalization of the method of Ref. 10 for circular geometries has been developed in Ref. 14. By substituting the functional (4) in Eqs. (1)–(3), we can rewrite the TDGL equations as follows:

$$\begin{aligned}\frac{\hbar^2}{2m_d^*D}\left(\frac{\partial}{\partial t} + \frac{ie^*}{\hbar}\varphi\right)\psi_d = &-\frac{1}{2m_d^*}\mathbf{\Pi}^2\psi_d - \frac{1}{2m_v^*}(\Pi_y^2 - \Pi_x^2)\psi_s \\ &+\alpha_d\psi_d - 2\beta_2|\psi_d|^2\psi_d - \beta_3|\psi_s|^2\psi_d - 2\beta_4\psi_s^2\bar{\psi}_d, \end{aligned} \tag{5}$$

$$\begin{aligned}\frac{\hbar^2}{2m_s^*D}\left(\frac{\partial}{\partial t} + \frac{ie^*}{\hbar}\varphi\right)\psi_s = &-\frac{1}{2m_s^*}\mathbf{\Pi}^2\psi_s - \frac{1}{2m_v^*}(\Pi_y^2 - \Pi_x^2)\psi_d \\ &+\alpha_s\psi_s - 2\beta_1|\psi_s|^2\psi_s - \beta_3|\psi_d|^2\psi_s - 2\beta_4\psi_d^2\bar{\psi}_s, \end{aligned} \tag{6}$$

$$\frac{4\pi\sigma}{c}\left(\frac{1}{c}\frac{\partial\mathbf{A}}{\partial t} + \nabla\varphi\right) = \frac{4\pi}{c}\mathbf{J}_s - \nabla\times\mathbf{B}, \tag{7}$$

where the *superconducting current density* is defined by

$$\begin{aligned}\mathbf{J}_s = &\frac{e^*}{m_d^*}\mathrm{Re}\left(\bar{\psi}_d\mathbf{\Pi}\psi_d\right) + \frac{e^*}{m_s^*}\mathrm{Re}\left(\bar{\psi}_s\mathbf{\Pi}\psi_s\right) - \frac{e^*}{m_v^*}\mathrm{Re}\left(\bar{\psi}_d\Pi_x\psi_s + \bar{\psi}_s\Pi_x\psi_d\right)\hat{x} \\ &+\frac{e^*}{m_v^*}\mathrm{Re}\left(\bar{\psi}_d\Pi_y\psi_s + \bar{\psi}_s\Pi_y\psi_d\right)\hat{y}; \end{aligned} \tag{8}$$

where Re indicates the real part of a complex function.

A very simple inspection of Eqs. (5)–(8) shows us that they are invariant under the *gauge transformation* $\psi_d' = \psi_d e^{i\chi}$, $\psi_s' = \psi_s e^{i\chi}$, $\mathbf{A}' = \mathbf{A} + \frac{\hbar c}{e^*}\nabla\chi$, $\varphi' = \varphi - \frac{\hbar}{e^*}\frac{\partial\chi}{\partial t}$. We will consider the particular gauge $\varphi' = 0$ at all times. It is not difficult to recover the numerical approximations of

This article is copyrighted as indicated in the article. Reuse of AIP content is subject to the terms at: http://scitation.aip.org/termsconditions. Downloaded to IP: 186.217.234.103 On: Fri, 10 Oct 2014 16:39:20

the TDGL equations for the most general gauge $\varphi' \neq 0$. Then, if we neglect the primes, the new equations can be simplified to

$$\frac{\hbar^2}{2m_d^* D}\frac{\partial \psi_d}{\partial t} = -\frac{1}{2m_d^*}\mathbf{\Pi}^2\psi_d - \frac{1}{2m_v^*}(\Pi_y^2 - \Pi_x^2)\psi_s + \alpha_d\psi_d - 2\beta_2|\psi_d|^2\psi_d - \beta_3|\psi_s|^2\psi_d - 2\beta_4\psi_s^2\bar{\psi}_d, \tag{9}$$

$$\frac{\hbar^2}{2m_s^* D}\frac{\partial \psi_s}{\partial t} = -\frac{1}{2m_s^*}\mathbf{\Pi}^2\psi_s - \frac{1}{2m_v^*}(\Pi_y^2 - \Pi_x^2)\psi_d + \alpha_s\psi_s - 2\beta_1|\psi_s|^2\psi_s - \beta_3|\psi_d|^2\psi_s - 2\beta_4\psi_d^2\bar{\psi}_s, \tag{10}$$

$$\frac{4\pi\sigma}{c^2}\frac{\partial \mathbf{A}}{\partial t} = \frac{4\pi}{c}\mathbf{J}_s - \nabla \times \mathbf{B}. \tag{11}$$

For simplicity, we will develop an algorithm to solve the TDGL equations on a two-dimensional rectangular domain. The generalization to the three-dimensional case is straightforward. Thus, we take all functions invariant along the z axis. Within this scenario, $\psi_d = \psi_d(x, y)$, $\psi_s = \psi_s(x, y)$, $\mathbf{B} = B_z(x, y)\mathbf{k}$, and $\mathbf{A} = A_x(x, y)\mathbf{i} + A_y(x, y)\mathbf{j}$.

Let us denote by Ω_{sc} the superconducting region. The outer medium can be either a metal or vacuum. Let $\partial\Omega_{sc}$ be the interface separating the superconducting from the outer medium. Solving Eqs. (9)–(11) requires known boundary conditions at the interface $\partial\Omega_{sc}$. Let us denote by $\mathbf{n}$ the unit vector outward normal to the interface. At $\partial\Omega_{sc}$ we impose that

$$\mathbf{J}_s \cdot \mathbf{n} = 0, \tag{12}$$

which is valid for a superconductor-vacuum interface. Had we used a superconductor-metal interface would be rather different.[15]

This condition gives the values of the order parameter components at the surface $\partial\Omega_{sc}$. We need an additional boundary condition for the induction. Let us denote by H the applied magnetic field. Then, at the interface $\partial\Omega_{sc}$,

$$B_z = H, \tag{13}$$

or equivalently,

$$(\nabla \times \mathbf{A})_z = H. \tag{14}$$

Therefore, solving Eqs. (9)–(11) subjected to the boundary conditions (12)–(14) is a well posed problem.

II. DIMENSIONLESS FORM OF THE TDGL EQUATIONS

For numerical purposes, it is more convenient to write the TDGL equations (9)–(11) in dimensionless units. Let us first consider the situation in which the system is not perturbed, that is, there is no applied magnetic field nor an applied current, i.e., both φ and $\mathbf{A}$ are zeroed. In that case, both components of the order parameter are constant everywhere and have no time dependence. Consequently, they are the solution of the equations $\frac{\delta\mathscr{L}}{\delta\bar{\psi}_d} = \frac{\delta\mathscr{L}}{\delta\bar{\psi}_s} = 0$, which produce

$$\alpha_d\psi_d - 2\beta_2|\psi_d|^2\psi_d - \beta_3|\psi_s|^2\psi_d - 2\beta_4\psi_s^2\bar{\psi}_d = 0, \tag{15}$$

$$\alpha_s\psi_s - 2\beta_1|\psi_s|^2\psi_s - \beta_3|\psi_d|^2\psi_s - 2\beta_4\psi_d^2\bar{\psi}_s = 0. \tag{16}$$

We can have three possible solutions; (a) $\psi_d \neq 0$ and $\psi_s = 0$; (b) $\psi_d = 0$ and $\psi_s \neq 0$; (c) $\psi_d \neq 0$ and $\psi_s \neq 0$. We will be most concerned with the first case in which the superconductor is nearly in the pure d-wave state deep inside the bulk. By considering the order parameter real, we obtain $\psi_d^2 = \psi_{d0}^2 = \frac{\alpha_d}{2\beta_2}$ and $\psi_s = 0$. This solution for the order parameters is the so-called pure *Meissner state*.

This article is copyrighted as indicated in the article. Reuse of AIP content is subject to the terms at: http://scitation.aip.org/termsconditions. Downloaded to IP: 186.217.234.103 On: Fri, 10 Oct 2014 16:39:20

If we multiply both sides of Eqs. (9) and (10) by ψ_{d0}, and substitute $\psi_d = \tilde{\psi}_d \psi_{d0}$, $\psi_s = \tilde{\psi}_s \psi_{d0}$, lead directly to the dimensionless quantities

- $\tau_1 = \frac{\beta_1}{\beta_2}$, $\tau_3 = \frac{\beta_3}{\beta_2}$, $\tau_4 = \frac{\beta_4}{\beta_2}$,
- $\eta_v = \frac{m_d^*}{m_v^*}$, $\eta_s = \frac{m_d^*}{m_s^*}$, $\nu = \frac{\alpha_s}{\alpha_d}$,
- $\beta = \frac{4\pi\sigma\kappa_d^2 D}{c^2}$,

and the following change of variables:

- $\nabla = \frac{1}{\xi_d}\tilde{\nabla}$, $t = \frac{\xi_d^2}{D}\tilde{t}$,
- $\mathbf{A} = H_{c2}\xi_d \tilde{\mathbf{A}}$, $\mathbf{B} = H_{c2}\tilde{\mathbf{B}}$,

where

- $\xi_d^2 = \frac{\hbar^2}{2m_d^*\alpha_d}$, $\lambda_d^2 = \frac{m_d^* c^2 \beta_2}{2\pi(e^*)^2\alpha_d}$, $\kappa_d = \frac{\lambda_d}{\xi_d}$,
- $\Phi_0 = \frac{hc}{2e}$, $H_{c2} = \frac{\Phi_0}{2\pi\xi_d^2}$.

As a result, we obtain the following dimensionless form of the TDGL equations:

$$\frac{\partial\tilde{\psi}_d}{\partial\tilde{t}} = -\tilde{\mathbf{\Pi}}^2\tilde{\psi}_d - \eta_v(\tilde{\Pi}_y^2 - \tilde{\Pi}_x^2)\tilde{\psi}_s + \tilde{\psi}_d - |\tilde{\psi}_d|^2\tilde{\psi}_d - \frac{\tau_3}{2}|\tilde{\psi}_s|^2\tilde{\psi}_d - \tau_4\tilde{\psi}_s^2\bar{\tilde{\psi}}_d, \tag{17}$$

$$\eta_s\frac{\partial\tilde{\psi}_s}{\partial\tilde{t}} = -\eta_s\tilde{\mathbf{\Pi}}^2\tilde{\psi}_s - \eta_v(\tilde{\Pi}_y^2 - \tilde{\Pi}_x^2)\tilde{\psi}_d + \nu\tilde{\psi}_s - \tau_1|\tilde{\psi}_s|^2\tilde{\psi}_s - \frac{\tau_3}{2}|\tilde{\psi}_d|^2\tilde{\psi}_s - \tau_4\tilde{\psi}_d^2\bar{\tilde{\psi}}_s, \tag{18}$$

$$\beta\frac{\partial\tilde{\mathbf{A}}}{\partial\tilde{t}} = \tilde{\mathbf{J}}_s - \kappa_d^2\tilde{\nabla}\times\tilde{\mathbf{B}}, \tag{19}$$

$$\tilde{\mathbf{J}}_s = \mathrm{Re}\left(\bar{\tilde{\psi}}_d\tilde{\mathbf{\Pi}}\tilde{\psi}_d\right) + \eta_s\mathrm{Re}\left(\bar{\tilde{\psi}}_s\tilde{\mathbf{\Pi}}\tilde{\psi}_s\right) - \eta_v\left[\mathrm{Re}\left(\bar{\tilde{\psi}}_d\tilde{\Pi}_x\tilde{\psi}_s + \bar{\tilde{\psi}}_s\tilde{\Pi}_x\tilde{\psi}_d\right)\right]\hat{x} + \eta_v\left[\mathrm{Re}\left(\bar{\tilde{\psi}}_d\tilde{\Pi}_y\tilde{\psi}_s + \bar{\tilde{\psi}}_s\tilde{\Pi}_y\tilde{\psi}_d\right)\right]\hat{y}, \tag{20}$$

where now $\tilde{\mathbf{\Pi}} = -i\tilde{\nabla} - \tilde{\mathbf{A}}$.

Here, ξ_d is the *coherence length* and λ_d is the *London penetration length*, the characteristic lengthscales for the spatial evolution of $|\psi_d|$ and $\mathbf{B}$, respectively; κ_d is then the *Ginzburg-Landau parameter* which is material dependent; H_{c2} is the upper critical field at which bulk superconductivity is destroyed.

From this point on, we will omit the tildes in all variables, for simplicity of the presented formulae.

III. THE AUXILIARY ORDER PARAMETERS

In order to solve the TDGL equations (17)–(19), it is convenient to rewrite them using auxiliary order parameters. Let us define

$$\Lambda = \psi_d - \eta_v\psi_s, \tag{21}$$

$$\lambda = \psi_d + \eta_v\psi_s, \tag{22}$$

$$\gamma = \eta_s\psi_s - \eta_v\psi_d, \tag{23}$$

$$\Gamma = \eta_s\psi_s + \eta_v\psi_d. \tag{24}$$

This article is copyrighted as indicated in the article. Reuse of AIP content is subject to the terms at: http://scitation.aip.org/termsconditions. Downloaded to IP: 186.217.234.103 On: Fri, 10 Oct 2014 16:39:20

Consequently, Eqs. (17)–(18) and (20) can be written as

$$\frac{\partial \psi_d}{\partial t} = -\Pi_x^2 \Lambda - \Pi_y^2 \lambda + \psi_d - |\psi_d|^2 \psi_d - \frac{\tau_3}{2}|\psi_s|^2 \psi_d - \tau_4 \psi_s^2 \bar{\psi}_d, \tag{25}$$

$$\eta_s \frac{\partial \psi_s}{\partial t} = -\Pi_x^2 \gamma - \Pi_y^2 \Gamma + \nu \psi_s - \tau_1 |\psi_s|^2 \psi_s - \frac{\tau_3}{2}|\psi_d|^2 \psi_s - \tau_4 \psi_d^2 \bar{\psi}_s, \tag{26}$$

$$J_{sx} = \mathrm{Re}\left[\bar{\psi}_d (\Pi_x \Lambda) + \bar{\psi}_s \Pi_x \gamma\right], \tag{27}$$

$$J_{sy} = \mathrm{Re}\left[\bar{\psi}_d (\Pi_y \lambda) + \bar{\psi}_s \Pi_y \Gamma\right]. \tag{28}$$

Equation (19) remains unchanged after introducing these new functions. This procedure hugely simplifies the implementation of the boundary conditions (12) in the sense that now we have conventional Neumann boundary conditions for the auxiliary order parameters. In fact, by supposing that both components of the order parameters are non-vanishing at the edge, in order to satisfy (12) we must have

$$\Pi_x \Lambda = 0, \ \Pi_x \gamma = 0, \ \text{at the west and east boundaries,} \tag{29}$$

$$\Pi_y \lambda = 0, \ \Pi_y \Gamma = 0, \ \text{at the south and north boundaries.} \tag{30}$$

Written in terms of the covariant derivative operator, it is not obvious that Eqs. (29)–(30) are Neumann boundary conditions. However, it will be shown in Sec. IV that this is indeed the case when we introduce the auxiliary field into the TDGL equations.

From (20) one notices that homogeneous Neumann boundary conditions for the d and s components of the order parameter, $\Pi_x \psi_d = \Pi_x \psi_s = 0$ at the west and east boundaries and $\Pi_y \psi_s = \Pi_y \psi_d = 0$, will result in vanishing of the current density perpendicular to the surface $\partial\Omega_{sc}$. However, this is a sufficient condition, but not a necessary one to make $\mathbf{J} \cdot \mathbf{n} = 0$ at $\partial\Omega_{sc}$. This is one of the aspects that differentiate the present method of solving the TDGL equations with respect to previous works (see, for instance, Refs. 9, 22, and 23). In other words, we require the weaker boundary conditions (29) and (30) to vanish the perpendicular current density at the boundaries. Maybe, for $(d + s)$-wave superconductors these two different sets of boundary conditions will not have much impact on the physics of the problem. However, for p-wave superconductors, which are very non-conventional, where we have mixed covariant derivative terms in the TDGL equations, the use of the auxiliary order parameters makes a great difference.[24]

The properties of the TDGL equations for a d-wave superconductor have been studied earlier in Ref. 7. There, a detailed mathematical analysis of these equations was made, and some approximations in the $\kappa_d \to \infty$ limit were devised. However, a clear algorithm to solve these equations, which can be easily implemented numerically, was not proposed. In addition, to our best knowledge, the introduction of the auxiliary order parameter presented above is novel as well and has significant advantages in solving the TDGL equations (in addition to those mentioned for the boundary conditions) which will be discussed through Secs. IV–VIII.

IV. AUXILIARY FIELDS

As a next step, we will introduce the auxiliary field vector $\mathbf{U} = (\mathcal{U}_x, \mathcal{U}_y)$ which is given by

$$\mathcal{U}_x(x, y, t) = \exp\left(-i \int_{x_0}^{x} A_x(\xi, y, t)\, d\xi\right),$$

$$\mathcal{U}_y(x, y, t) = \exp\left(-i \int_{y_0}^{y} A_y(x, \eta, t)\, d\eta\right), \tag{31}$$

where (x_0, y_0) is an arbitrary reference point. From now on, we will assume that the time dependence is implicit in all functions.

This has become a very common procedure in the numerical treatment of the conventional Ginzburg-Landau equations.[16] The main idea behind this technique is to guarantee that the discretization of the TDGL equations preserves gauge invariance.[10,11] Otherwise, one may obtain

This article is copyrighted as indicated in the article. Reuse of AIP content is subject to the terms at: http://scitation.aip.org/termsconditions. Downloaded to IP: 186.217.234.103 On: Fri, 10 Oct 2014 16:39:20

undesirable non-physical solutions. Another advantage is that, by incorporating this field into the conventional TDGL equation for the order parameter, we obtain an equation which resembles a diffusion equation, the discretization of which has a very well defined stability criterion.

The auxiliary field has the following properties:

$$\Pi_j f = -i\bar{\mathcal{U}}_j \frac{\partial(\mathcal{U}_j f)}{\partial x_j}, \tag{32}$$

$$\Pi_j^2 f = -\bar{\mathcal{U}}_j \frac{\partial^2(\mathcal{U}_j f)}{\partial x_j^2}, \tag{33}$$

with $(x_1, x_2) = (x, y)$ and $\{j = 1, 2\}$. Upon taking (32) into (27) and (28), the current density components become

$$J_{sx} = \mathrm{Im}\left[\bar{\mathcal{U}}_x \bar{\psi}_d \frac{\partial(\mathcal{U}_x \Lambda)}{\partial x} + \bar{\mathcal{U}}_x \bar{\psi}_s \frac{\partial(\mathcal{U}_x \gamma)}{\partial x}\right], \tag{34}$$

$$J_{sy} = \mathrm{Im}\left[\bar{\mathcal{U}}_y \bar{\psi}_d \frac{\partial(\mathcal{U}_y \lambda)}{\partial y} + \bar{\mathcal{U}}_y \bar{\psi}_s \frac{\partial(\mathcal{U}_y \Gamma)}{\partial y}\right], \tag{35}$$

where Im denotes the imaginary part of a complex function. It is now clear that the boundary conditions (29) and (30) are of Neumann type,

$$\frac{\partial(\mathcal{U}_x \Lambda)}{\partial x} = 0, \quad \frac{\partial(\mathcal{U}_x \gamma)}{\partial x} = 0, \text{ at the west and east boundaries,} \tag{36}$$

$$\frac{\partial(\mathcal{U}_y \lambda)}{\partial y} = 0, \quad \frac{\partial(\mathcal{U}_y \Gamma)}{\partial y} = 0, \text{ at the south and north boundaries.} \tag{37}$$

Next, we substitute Eqs. (33) into (25) and (26) to obtain

$$\begin{aligned} \frac{\partial \psi_d}{\partial t} &= \bar{\mathcal{U}}_x \frac{\partial^2 (\mathcal{U}_x \Lambda)}{\partial x^2} + \bar{\mathcal{U}}_y \frac{\partial^2 (\mathcal{U}_y \lambda)}{\partial y^2} \\ &\quad + \psi_d - |\psi_d|^2 \psi_d - \frac{\tau_3}{2} |\psi_s|^2 \psi_d - \tau_4 \psi_s^2 \bar{\psi}_d, \end{aligned} \tag{38}$$

$$\begin{aligned} \eta_s \frac{\partial \psi_s}{\partial t} &= \bar{\mathcal{U}}_x \frac{\partial^2 (\mathcal{U}_x \gamma)}{\partial x^2} + \bar{\mathcal{U}}_y \frac{\partial^2 (\mathcal{U}_y \Gamma)}{\partial y^2} \\ &\quad + \nu \psi_s - \tau_1 |\psi_s|^2 \psi_s - \frac{\tau_3}{2} |\psi_d|^2 \psi_s - \tau_4 \psi_d^2 \bar{\psi}_s. \end{aligned} \tag{39}$$

In Secs. V and VI, we will develop an algorithm to solve Eqs. (19), (38), and (39) numerically, subjected to the boundary conditions (36) and (37), with the current density given by (34)–(35) and (13)–(14).

V. COMPUTATIONAL GRID

The computational grid which will be used to find the best approximation for the TDGL equations is illustrated in Figure 1. It is a domain comprehended by a rectangle of $N_x \times N_y$ unit cells of size $(\Delta x, \Delta y)$ in the x and y directions, respectively. Then, the vertex points in the mesh are given by $\{x_i = (i - 1)\Delta x, y_j = (j - 1)\Delta y, i = 1, 2, \ldots, N_x + 1, j = 1, 2, \ldots, N_y + 1\}$. The superconducting domain is given by

$$\Omega_{sc} = \left\{\mathbf{r} = (x, y) : x_1 + \frac{\Delta x}{2} < x < x_{N_x} + \frac{\Delta x}{2}, y_1 + \frac{\Delta y}{2} < y < y_{N_y} + \frac{\Delta y}{2}\right\}. \tag{40}$$

This article is copyrighted as indicated in the article. Reuse of AIP content is subject to the terms at: http://scitation.aip.org/termsconditions. Downloaded to IP: 186.217.234.103 On: Fri, 10 Oct 2014 16:39:20

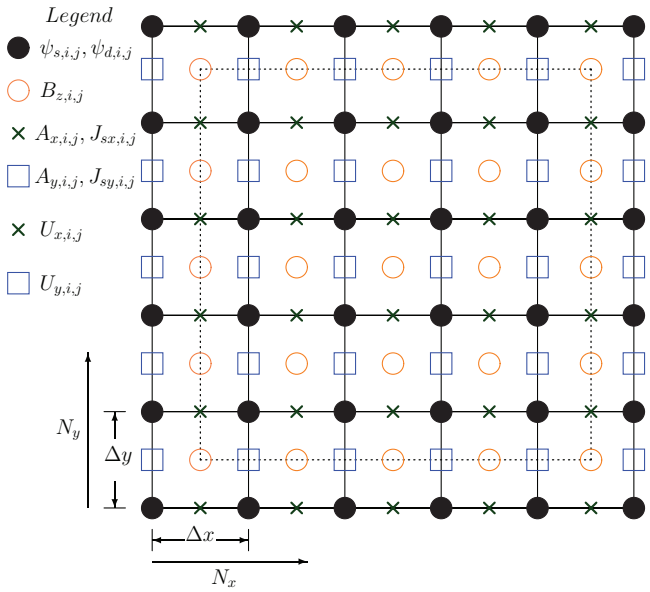

FIG. 1. The computational grid used for the discretization of the TDGL equations. The superconducting domain Ω_{sc} is limited by the dashed line $\partial\Omega_{sc}$; the true meaning of the dashed line is explained in the text. The points where each quantity is calculated are indicated in the legend.

The superconducting region is surrounded by a conveniently attached thin superconducting layer of width $\frac{\Delta x}{2}$ in the horizontal direction and $\frac{\Delta y}{2}$ in the vertical direction. Both regions are inside the domain

$$\Omega = \left\{\mathbf{r} = (x, y) : \; x_1 < x < x_{N_x+1}, y_1 < y < y_{N_y+1}\right\}. \tag{41}$$

We denote by $\partial\Omega_{sc}$ the interface between the superconductor and the added superconducting layer (dashed line in Figure 1), and by $\partial\Omega$ the superconducting layer-vacuum interface. The boundary conditions will be employed at the $\partial\Omega_{sc}$ interface rather than $\partial\Omega$. The actual superconducting-vacuum interface is Ω_{sc}. The edge $\partial\Omega$ is constituted only by *ghost-points* used only for illustration purposes of the order parameter. As it will be seen later on, the values of the order parameter in the domain Ω_{sc} do not depend on the values of (ψ_d, ψ_s) at the edges.

VI. DISCRETIZATION OF THE TDGL EQUATIONS

We are now in position to initialize the discretization of the TDGL equations. Before that, let us consider the product of the auxiliary field $\mathcal{U}_x$ between two consecutive points (x_i, y_j) and (x_{i+1}, y_j)

$$\begin{aligned} U_{x,i,j} &\equiv \bar{\mathcal{U}}_x(x_i, y_j)\mathcal{U}_x(x_{i+1}, y_j) \\ &= \exp\left(-i\int_{x_i}^{x_{i+1}} A_x dx\right) \\ &= \exp\left(-i A_{x,i,j}\Delta x\right), \end{aligned} \tag{42}$$

where we have used the middle point rule for integration. Similarly, we have

$$\begin{aligned} U_{y,i,j} &\equiv \bar{\mathcal{U}}_y(x_i, y_j)\mathcal{U}_y(x_i, y_{j+1}) \\ &= \exp\left(-i A_{y,i,j}\Delta y\right), \end{aligned} \tag{43}$$

where $A_{x,i,j} \equiv A_x(x_i + \frac{\Delta x}{2}, y_j)$ and $A_{y,i,j} \equiv A_y(x_i, y_j + \frac{\Delta y}{2})$. Thus, it is clear that the *variables* $U_{x,i,j}$ and $U_{y,i,j}$ *link* the auxiliary field components at two adjacent points of the mesh through the vector potential in the middle point.

This article is copyrighted as indicated in the article. Reuse of AIP content is subject to the terms at: http://scitation.aip.org/termsconditions. Downloaded to IP: 186.217.234.103 On: Fri, 10 Oct 2014 16:39:20

The next step is to use the central difference formula for the second derivative and Definition (42). We have,

$$\bar{\mathcal{U}}_x \frac{\partial^2}{\partial x^2}(\mathcal{U}_x \Lambda)\Big|_{(x_i,y_j)} = \frac{U_{x,i,j}\Lambda_{i+1,j} - 2\Lambda_{i,j} + \bar{U}_{x,i-1,j}\Lambda_{i-1,j}}{\Delta x^2}, \tag{44}$$

where $\Lambda(x_i, y_j) \equiv \Lambda_{i,j}$. Similar result can be obtained for the derivative with respect to the y coordinate involving the functions $\mathcal{U}_y$ and λ. Therefore, the discrete version of Eqs. (38) and (39) is

$$\frac{\partial \psi_{d,i,j}}{\partial t} = \mathscr{D}_{i,j}, \tag{45}$$

$$\eta_s \frac{\partial \psi_{s,i,j}}{\partial t} = \mathscr{S}_{i,j}, \tag{46}$$

where

$$\begin{aligned}\mathscr{D}_{i,j} = &\frac{U_{x,i,j}\Lambda_{i+1,j} - 2\Lambda_{i,j} + \bar{U}_{x,i-1,j}\Lambda_{i-1,j}}{\Delta x^2} \\ &+\frac{U_{y,i,j}\lambda_{i,j+1} - 2\lambda_{i,j} + \bar{U}_{y,i,j-1}\lambda_{i,j-1}}{\Delta y^2} \\ &+\psi_{d,i,j} - |\psi_{d,i,j}|^2\psi_{d,i,j} - \frac{\tau_3}{2}|\psi_{s,i,j}|^2\psi_{d,i,j} - \tau_4\psi_{s,i,j}^2\bar{\psi}_{d,i,j},\end{aligned} \tag{47}$$

$$\begin{aligned}\mathscr{S}_{i,j} = &\frac{U_{x,i,j}\gamma_{i+1,j} - 2\gamma_{i,j} + \bar{U}_{x,i-1,j}\gamma_{i-1,j}}{\Delta x^2} \\ &+\frac{U_{y,i,j}\Gamma_{i,j+1} - 2\Gamma_{i,j} + \bar{U}_{y,i,j-1}\Gamma_{i,j-1}}{\Delta y^2} \\ &+\nu\psi_{s,i,j} - \tau_1|\psi_{s,i,j}|^2\psi_{s,i,j} - \frac{\tau_3}{2}|\psi_{d,i,j}|^2\psi_{s,i,j} - \tau_4\psi_{d,i,j}^2\bar{\psi}_{s,i,j},\end{aligned} \tag{48}$$

for all $\{i = 2, \ldots, N_x, j = 2, \ldots, N_y\}$. Here, $\lambda(x_i, y_j) \equiv \lambda_{i,j}$, $\gamma(x_i, y_j) \equiv \gamma_{i,j}$, $\Gamma(x_i, y_j) \equiv \Gamma_{i,j}$, $\psi_d(x_i, y_j) \equiv \psi_{d,i,j}$, and $\psi_s(x_i, y_j) \equiv \psi_{s,i,j}$.

At this point, we can see another advantage of introducing the auxiliary order parameters. The discrete Laplacian in (47) and (48) would have three times as much terms if we had discretized the original equations (17) and (18). The same will occur with current density components. From the computational point of view, this is very costly.

Let us now discretize the current density components (34) and (35). First, we use the central difference formula to evaluate $\frac{\partial(\mathcal{U}_x\Lambda)}{\partial x}\Big|_{(x_i+\frac{\Delta x}{2},y_j)}$. Second, we approximate $\bar{\mathcal{U}}_x\bar{\psi}_d$ at $(x_i + \frac{\Delta x}{2}, y_i)$ by its average value at the nearest vertex points in the mesh. Then, using Definition (42) of the link variable, we are left with

$$\begin{aligned}J_{sx,i,j} &\equiv J_{sx}(x_i + \frac{\Delta x}{2}, y_j) \\ &= \frac{1}{2\Delta x}\mathrm{Im}\left\{\left[\bar{U}_{x,i,j}\bar{\psi}_{d,i+1,j} + \bar{\psi}_{d,i,j}\right]\left[U_{x,i,j}\Lambda_{i+1,j} - \Lambda_{i,j}\right]\right. \\ &\quad \left.+\left[\bar{U}_{x,i,j}\bar{\psi}_{s,i+1,j} + \bar{\psi}_{s,i,j}\right]\left[U_{x,i,j}\gamma_{i+1,j} - \gamma_{i,j}\right]\right\},\end{aligned} \tag{49}$$

for all $\{i = 1, 2, \ldots, N_x, j = 1, 2, \ldots, N_y + 1\}$. Similarly,

$$\begin{aligned}J_{sy,i,j} &= J_{sy}(x_i, y_j + \frac{\Delta y}{2}) \\ &= \frac{1}{2\Delta y}\mathrm{Im}\left\{\left[\bar{U}_{y,i,j}\bar{\psi}_{d,i,j+1} + \bar{\psi}_{d,i,j}\right]\left[U_{y,i,j}\lambda_{i,j+1} - \lambda_{i,j}\right]\right. \\ &\quad \left.+\left[\bar{U}_{y,i,j}\bar{\psi}_{s,i,j+1} + \bar{\psi}_{s,i,j}\right]\left[U_{y,i,j}\Gamma_{i,j+1} - \Gamma_{i,j}\right]\right\},\end{aligned} \tag{50}$$

for all $\{i = 1, 3, \ldots, N_x + 1, j = 1, 2, \ldots, N_y\}$.

This article is copyrighted as indicated in the article. Reuse of AIP content is subject to the terms at: http://scitation.aip.org/termsconditions. Downloaded to IP: 186.217.234.103 On: Fri, 10 Oct 2014 16:39:20

We still have to discretize the equation for the vector potential (19). Taking into account that $\mathbf{B} = B_z\mathbf{k}$, we have

$$\beta\frac{\partial A_x}{\partial t} = J_{sx} - \kappa_d^2\frac{\partial B_z}{\partial y}, \tag{51}$$

$$\beta\frac{\partial A_y}{\partial t} = J_{sy} + \kappa_d^2\frac{\partial B_z}{\partial x}. \tag{52}$$

The discrete form of these equations are

$$\beta\frac{\partial A_{x,i,j}}{\partial t} = J_{sx,i,j} - \frac{\kappa_d^2}{\Delta y}(B_{z,i,j} - B_{z,i,j-1}), \tag{53}$$

for all $\{i = 1, 2, \ldots, N_x, j = 2, 3, \ldots, N_y\}$, and

$$\beta\frac{\partial A_{y,i,j}}{\partial t} = J_{sy,i,j} + \frac{\kappa_d^2}{\Delta x}(B_{z,i,j} - B_{z,i-1,j}), \tag{54}$$

for all $\{i = 2, 3, \ldots, N_x, j = 1, 2, \ldots, N_y\}$, where $B_{z,i,j} \equiv B_z(x_i + \frac{\Delta x}{2}, y_j + \frac{\Delta y}{2})$.

To finalize the discretization of the TDGL equations, we need an approximation for the induction. From the central difference formula for the first derivative, it is not difficult to see that the discrete form of $B_z = \partial A_y/\partial x - \partial A_x/\partial y$ is

$$B_{z,i,j} = \frac{A_{y,i+1,j} - A_{y,i,j}}{\Delta x} - \frac{A_{x,i,j+1} - A_{y,i,j-1}}{\Delta y}, \tag{55}$$

for all $\{i = 2, 3, \ldots, N_x - 1, j = 2, \ldots, N_y - 1\}$.

Let us denote the discrete time by $t_n = (n - 1)\Delta t$ for all $\{n = 1, 2, \ldots\}$, and $f_n \equiv f(t_n)$. Then, by using the first order approximation

$$\int_{t_n}^{t_{n+1}} f(t)dt = f_n\Delta t, \tag{56}$$

from Eqs. (45)–(46) and (53)–(54), we obtain the following set of recursive relations:

$$\psi_{d,i,j}^{n+1} = \psi_{d,i,j}^n + \Delta t\mathscr{D}_{i,j}^n, \tag{57}$$

$$\psi_{s,i,j}^{n+1} = \psi_{s,i,j}^n + \frac{\Delta t}{\eta_s}\mathscr{S}_{i,j}^n, \tag{58}$$

$$A_{x,i,j}^{n+1} = A_{x,i,j}^n + \frac{\Delta t}{\beta}J_{sx,i,j} - \frac{\kappa_d^2}{\beta\Delta y}(B_{z,i,j}^n - B_{z,i,j-1}^n), \tag{59}$$

$$A_{y,i,j}^{n+1} = A_{y,i,j}^n + \frac{\Delta t}{\beta}J_{sy,i,j} + \frac{\kappa_d^2}{\beta\Delta x}(B_{z,i,j}^n - B_{z,i-1,j}^n). \tag{60}$$

To conclude the evaluation of all physical quantities at $t = t_{n+1}$, we need to determine them at the edge points by using the boundary conditions. We start from the induction. From (13), we have

$$B_{z,1,j} = H, \tag{61}$$

$$B_{z,Nx,j} = H, \tag{62}$$

$$B_{z,i,1} = H, \tag{63}$$

$$B_{z,i,Ny} = H, \tag{64}$$

for all $\{i = 1, 2, \ldots, N_x, j = 2, 3, \ldots, N_y - 1\}$.

A quick inspection of the recursion relations (59) and (60) leads to the conclusion that $(A_{x,1,j}, A_{x,N_x,j})$ and $(A_{y,i,1}, A_{y,i,N_y})$ remain constant at all times. To see this, we just note that $J_{sx,1,j} = J_{sx,N_x,j} = 0$ and $J_{sy,i,1} = J_{sy,i,N_y} = 0$ at all times, for all $\{j = 2, 3, \ldots, N_y\}$ and $\{i = 2, 3,$

This article is copyrighted as indicated in the article. Reuse of AIP content is subject to the terms at: http://scitation.aip.org/termsconditions. Downloaded to IP: 186.217.234.103 On: Fri, 10 Oct 2014 16:39:20

$\ldots, N_x\}$, respectively, which is required by the boundary condition (12). In addition, the induction is constant along the boundary. Notice also that to run all recursion relations we do not need the values of $(A_{x,i,1}, A_{x,i,N_y+1})$ and $(A_{y,1,j}, A_{y,N_x+1,j})$. However, we determine them from (55), where there is always only one unknown at the edges, except at the corners. This enables us to find the link variables at the edge points and consequently the components of the superconducting current density.

To end the discretization procedure, we need to discretize Eqs. (36) and (37). As before, we use the central difference approximation for the first derivative. We obtain

$$\Lambda_{1,j} = U_{x,1,j}\Lambda_{2,j}, \tag{65}$$

$$\gamma_{1,j} = U_{x,1,j}\gamma_{2,j}, \tag{66}$$

at the west boundary,

$$\Lambda_{N_x+1,j} = \bar{U}_{x,N_x,j}\Lambda_{N_x,j}, \tag{67}$$

$$\gamma_{N_x+1,j} = \bar{U}_{x,N_x,j}\gamma_{N_x,j}, \tag{68}$$

at the east boundary,

$$\Gamma_{i,1} = U_{y,i,1}\Gamma_{i,2}, \tag{69}$$

$$\lambda_{i,1} = U_{y,i,1}\lambda_{i,2}, \tag{70}$$

at the south boundary,

$$\Gamma_{i,N_y+1} = \bar{U}_{y,i,N_y}\Gamma_{i,N_y}, \tag{71}$$

$$\lambda_{i,N_y+1} = \bar{U}_{y,i,N_y}\lambda_{i,N_y}, \tag{72}$$

at the north boundary, for all times. We have asserted before that the inner values of the order parameter components do not depend on their outer values on $\partial\Omega$. Indeed, if we substitute (65) in (47) considering $i = 1$, we can immediately see that the first term of this last equation becomes $(U_{x,1,j}\Lambda_{2,j} - \Lambda_{2,j})/\Delta x^2$.

Hence, once we have determined the order parameter components from the recursive relations (57) and (58) inside the mesh points at the time $t = t_{n+1}$, we can determine the auxiliary order parameters from (21)–(24). Next, we determine the auxiliary order parameters at the boundaries using the above equations.

In summary, we briefly recapitulate how the algorithm works. If we know $(\psi_{d,i,j}, \psi_{s,i,j}, A_{x,i,j}, A_{y,i,j})$ at $t = t_n$, from Eqs. (21)–(24), (47)–(50), and (55) we can calculate all the quantities required to evaluate the right-hand side of (57)–(60) at the interior mesh points. Next, we evaluate the auxiliary order parameters from Eqs. (21)–(24). Finally, the boundary conditions are applied. Before going to the next time step, we update all relevant quantities like the link variables, current density, and the induction at all mesh points. By repeating this procedure we can determine all the relevant physical quantities at all times, until the system achieves the stationary state. Unfortunately, this method does not converge for an arbitrary time step Δt. We have used the following practical rule:

$$\Delta t \leq \min\left\{\frac{\delta^2}{4}, \frac{\delta^2\eta_s}{4}, \frac{\delta^2\beta}{4\kappa_d^2}\right\}, \tag{73}$$

$$\delta^2 = \frac{2}{\frac{1}{\Delta x^2} + \frac{1}{\Delta y^2}}, \tag{74}$$

which worked for all cases we have analyzed. This is another important characteristic of our strategy of introducing the auxiliary order parameters. Since transformations (21)–(24) make the Laplacian of the TDGL equations isotropic-like ones, as we can see from (38), the time step rule

This article is copyrighted as indicated in the article. Reuse of AIP content is subject to the terms at: http://scitation.aip.org/termsconditions. Downloaded to IP: 186.217.234.103 On: Fri, 10 Oct 2014 16:39:20

for multicomponent order parameter system is straightforward. This a crucial point to guarantee the stability towards the stationary state.

Notice that materials with high κ_d impose a limitation on the algorithm, which becomes very time consuming in order to obtain the stationary state, since the time step is small. In these cases, the implicit method of time integration should be used which are usually unconditionally convergent. However, for $\kappa_d \gg 1$ it is most convenient to consider the local magnetic field nearly constant everywhere and equals the applied field, that is, the vector potential is taken fixed as $\mathbf{A} = -\frac{Hy}{2}\mathbf{i} + \frac{Hx}{2}\mathbf{j}$. Then, we do not need to solve Eqs. (19), only for the order parameter components. In addition, the time step is smaller than the situation in which we keep κ_d large but finite. This approximation is quite good for $\kappa_d \geq 5$.[18]

VII. SOME PHYSICAL QUANTITIES

There are several important physical quantities in superconductivity which can be measured experimentally. One of them is the *average induction* which is defined as the spatial average of the induction,

$$\bar{B}_z = \frac{1}{S}\int\int_{\Omega} B_z(x, y)\, dx\, dy, \tag{75}$$

where S is the total area of the domain Ω. By using the midpoint rule for double integration, the discrete version of this definition can be written as

$$\bar{B}_z = \frac{1}{N_x N_y}\sum_{i=1}^{N_x}\sum_{j=1}^{N_y} B_{z,i,j}. \tag{76}$$

The second quantity is the *magnetization* which is a measure of the expelled magnetic field from the superconductor, and defined as

$$4\pi M = \bar{B}_z - H. \tag{77}$$

Third important quantity is the *Gibbs free-energy*. This energy is not measurable directly, but it can be obtained from the other two by using the *virial theorem*.[17] In dimensionless units, we have the following expression for the free-energy:

$$\begin{aligned} F = \frac{1}{A}\int\int \Big[& -\nu|\psi_s|^2 - |\psi_d|^2 + \frac{\tau_1}{2}|\psi_s|^4 + \frac{1}{2}|\psi_d|^4 + \frac{\tau_3}{2}|\psi_s|^2|\psi_d|^2 \\ & + \frac{\tau_4}{2}\left(\bar{\psi}_s^2\psi_d^2 + \bar{\psi}_d^2\psi_s^2\right) + |\boldsymbol{\Pi}\psi_d|^2 + \eta_s|\boldsymbol{\Pi}\psi_s|^2 \\ & + \eta_v\left(\bar{\Pi}_y\bar{\psi}_s\Pi_y\psi_d + \bar{\Pi}_y\bar{\psi}_d\Pi_y\psi_s - \bar{\Pi}_x\bar{\psi}_s\Pi_x\psi_d - \bar{\Pi}_x\bar{\psi}_d\Pi_x\psi_s\right) \\ & + \kappa_d^2(B_z - H)^2\Big]\, dx\, dy. \end{aligned} \tag{78}$$

The use of integration by parts, the boundary conditions (29) and (30), and finally the TDGL equations (17) and (18), in this sequence, yields for the stationary state

$$\begin{aligned} F = \frac{1}{A}\int\int \Big[& \kappa_d^2(B_z - H)^2 - \frac{\tau_1}{2}|\psi_s|^4 - \frac{1}{2}|\psi_d|^4 - \frac{\tau_3}{2}|\psi_s|^2|\psi_d|^2 \\ & - \frac{\tau_4}{2}\left(\bar{\psi}_s^2\psi_d^2 + \bar{\psi}_d^2\psi_s^2\right)\Big]\, dx\, dy, \end{aligned} \tag{79}$$

This article is copyrighted as indicated in the article. Reuse of AIP content is subject to the terms at: http://scitation.aip.org/termsconditions. Downloaded to IP: 186.217.234.103 On: Fri, 10 Oct 2014 16:39:20

or in the discrete form

$$F = \frac{1}{N_x N_y}\left\{\sum_{i=1}^{N_x}\sum_{j=1}^{N_y}\kappa_d^2(B_{z,i,j}-H)^2 - \sum_{i=2}^{N_x}\sum_{j=2}^{N_y}\left[\frac{\tau_1}{2}|\psi_{s,i,j}|^4+\frac{1}{2}|\psi_{d,i,j}|^4+\frac{\tau_3}{2}|\psi_{s,i,j}|^2|\psi_{d,i,j}|^2 + \frac{\tau_4}{2}\left(\bar{\psi}^2_{s,i,j}\psi^2_{d,i,j}+\bar{\psi}^2_{d,i,j}\psi^2_{s,i,j}\right)\right]\right\}. \quad (80)$$

VIII. COMPUTATIONAL RESULTS

The recursive relations supplemented by the boundary conditions derived in Sec. VII were implemented in Fortran 90 language.[25] We started from the Meissner state, taking $\psi_{d,i,j}=1$, $\psi_{s,i,j}=0$, $A_{x,i,j}=A_{y,i,j}=0$, $U_{x,i,j}=U_{y,i,j}=1$, and $B_{z,i,j}=0$ as the initial conditions in the entire sample. By keeping the external magnetic field H constant, we allow the system to evolve towards the stationary state. Next, we ramp up the applied field in increments of ΔH. The stationary solution for H is then used as the initial state to determine the solution for $H+\Delta H$, and so on. Usually we started from zero field and increased H until superconductivity was destroyed. For each field, we monitored the highest differences $|\psi_d^m-\psi_d^n|$ and $|\psi_s^m-\psi_s^n|$ for all vertex points in the mesh over a time interval typically of order $m-n\sim 10^3$. The largest difference smaller than the precision $\epsilon=10^{-5}$ was taken as the criterion to have obtained a stationary solution.

As an example of the application of the algorithm, we consider a superconducting square of dimensions $8\xi_d\times 8\xi_d$ with material parameters $\kappa_d=2$, $\tau_1=8/3$, $\tau_3=16/3$, $\tau_4=2$, $\nu=-2$, $\eta_s=2$, $\eta_v=1$; this value of ν corresponds to $\alpha_s/\alpha_{d0}=1$ and $T/T_c=0.5$. These parameters were taken from Ref. 2, where they were microscopically derived and used in a numerical simulation of an infinite $(d+s)$-wave superconductor by using periodic boundary conditions.[3] In Figure 2, we present the calculated magnetization and Gibbs free-energy as a function of the external applied field. First, we increased H adiabatically until the order parameter vanishes everywhere. Then we gradually decreased the field to zero (red dashed curve). As can be seen, calculated quantities exhibit a series of discontinuities, where each jump indicates a nucleation of one or more vortices inside the superconductor if H increases, or exit of vortices if H decreases. This is a very typical behavior of a mesoscopic superconductor, where states are labeled by vorticity L.[19] By *mesoscopic* we mean a superconductor of dimensions of order a few ξ_d.

Figure 2 also shows some other interesting features. For the considered mesoscopic superconductor, the upper critical field to destroy superconductivity is of order $H\approx 2H_{c2}(0)$ for a pure s-wave superconductor,[19,20] whereas for the $(d+s)$-wave we found it to be $H\approx 2.5H_{c2}(0)$, i.e., the superconducting critical parameters are enhanced by the mixing with a d-wave order parameter. Another interesting feature is that for $H=0$ we still have trapped flux inside the superconductor in decreasing H. This is quite remarkable, since we do not have any defect to which vortex pinning can be attributed and is a consequence of the presence of the surface barrier. Indeed, Figure 3 shows the order parameter for both components, and Figure 4 depicts the induction and the current distribution, also for $H=0$. As can be clearly seen from these figures, a single vortex remains at the center of the square in spite of the complete removal of the applied field. A possible explanation for these results is as follows. In the d-band what we have is a *vortex* and in the s-band an *anti-vortex*.[26] So there is an attractive interaction which keeps them together at the center of the sample. In fact, in Figure 5 we have plotted the current density vector field for both the d- and the s-vortex.[27] As we can clearly see, around the vortex core, the currents circulate in opposite direction (anticlockwise for the d-vortex and clockwise for the s-vortex). In other words, the currents are indeed countered, and thus minimize the energy when those vortices are on top of each other and currents compensate. We have learned that this is a rather weak effect. If we invert the field towards negative values, we noticed that the vortex remains stable only to very weak fields. This should be studied

This article is copyrighted as indicated in the article. Reuse of AIP content is subject to the terms at: http://scitation.aip.org/termsconditions. Downloaded to IP: 186.217.234.103 On: Fri, 10 Oct 2014 16:39:20

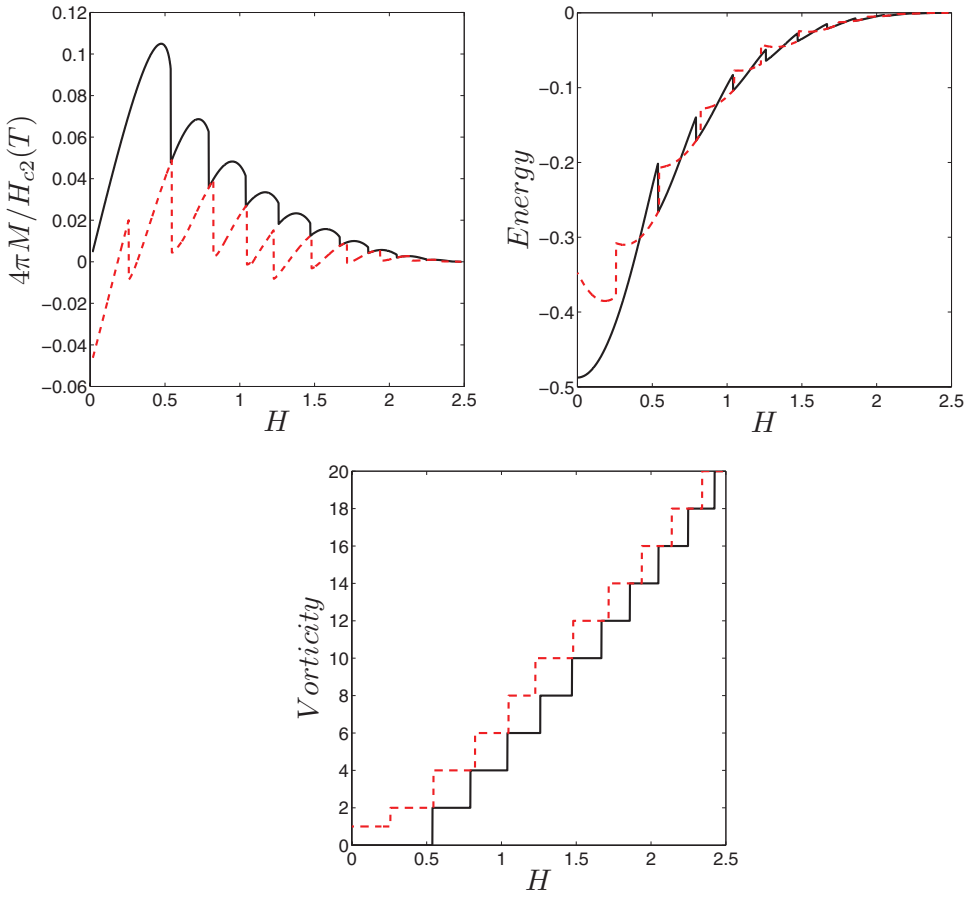

FIG. 2. The magnetization (upper-left) and the Gibbs free-energy (upper-right) as a function of the external applied field; for magnetic field sweeping up (black curve) and then down (red dashed curve). Different states are labeled by their corresponding vorticity L (lower panel).

further to see if it can be observed in realistic conditions (e.g., for corrugated sample surfaces and edges).

It is of course well known that the vortex configurations exhibit a very different behavior in mesoscopic superconductors compared to bulk superconductors. For a pure s-wave mesoscopic superconductor, confinement can lead to the formation of a giant vortex (two or more vortices coalescing into one).[19–21] We found that this also occurs for a mixed $(d + s)$-wave superconductor but in a rather different way. In the left panel of Figure 6, we show the density plot of $|\psi_d|$ for six vortices, just immediately after they nucleated inside the superconductor. As we increase H, the two central vortices move to the exact center of the sample forming a giant vortex (see right panel of the same figure). In a pure s-wave superconductor of the same size, this happens immediately after the vortices penetrate the sample, and, as more vortices penetrate the sample the giant vortex at the center increases in vorticity. However, our simulations show that the latter does not occur for a $(d + s)$-wave superconductor. In fact, in the left panel of Figure 7 we show the density plot of $|\psi_d|$ for $L = 8$, where it can be seen that the giant vortex at the center splits into individual vortices. To confirm this, in the right panel of the same figure we plotted $|\psi_d|$ in logarithmic scale, and we clearly observe that four vortices at the center are separated. We conclude that d-wave symmetry of the order parameter enhances the influence of the C_4 symmetry of the sample, having direct consequences on the vortex states.

This article is copyrighted as indicated in the article. Reuse of AIP content is subject to the terms at: http://scitation.aip.org/termsconditions. Downloaded to IP: 186.217.234.103 On: Fri, 10 Oct 2014 16:39:20

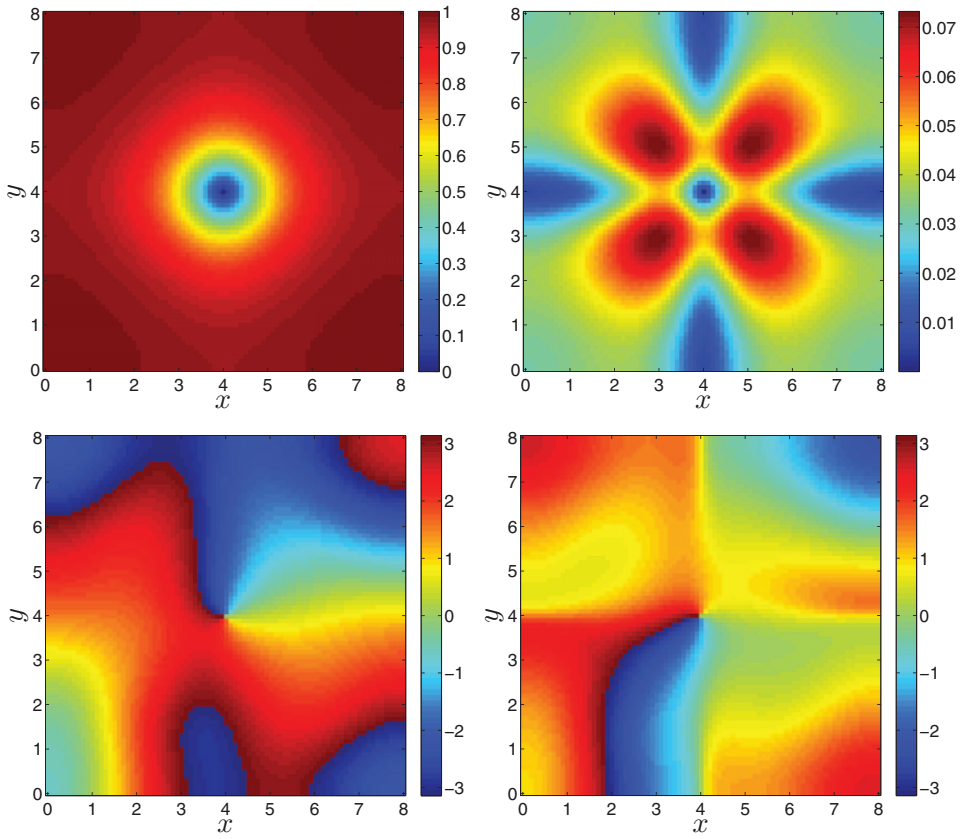

FIG. 3. Density plot of the order parameter for the *d*-component (upper-left) and the *s*-component (upper-right). Density plot of the phase of the *d*-component (down-left) and the *s*-component (down-right).

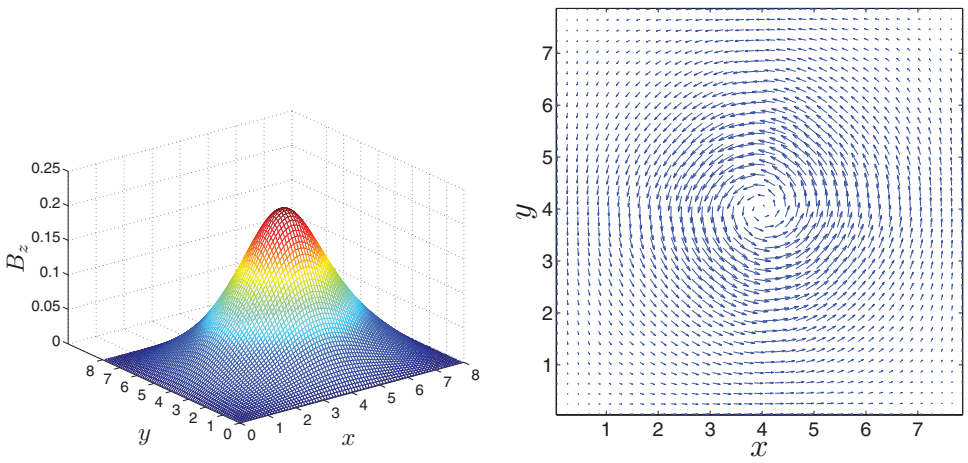

FIG. 4. The induction (left) and the current density vector field (right).

This article is copyrighted as indicated in the article. Reuse of AIP content is subject to the terms at: http://scitation.aip.org/termsconditions. Downloaded to IP: 186.217.234.103 On: Fri, 10 Oct 2014 16:39:20

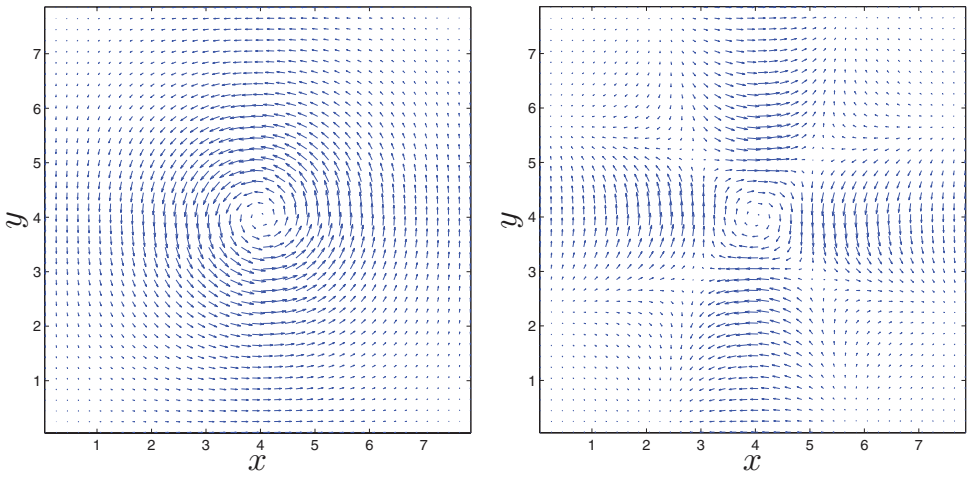

FIG. 5. The current density vector field for both the *d*-vortex (left) and the *s*-vortex (right).

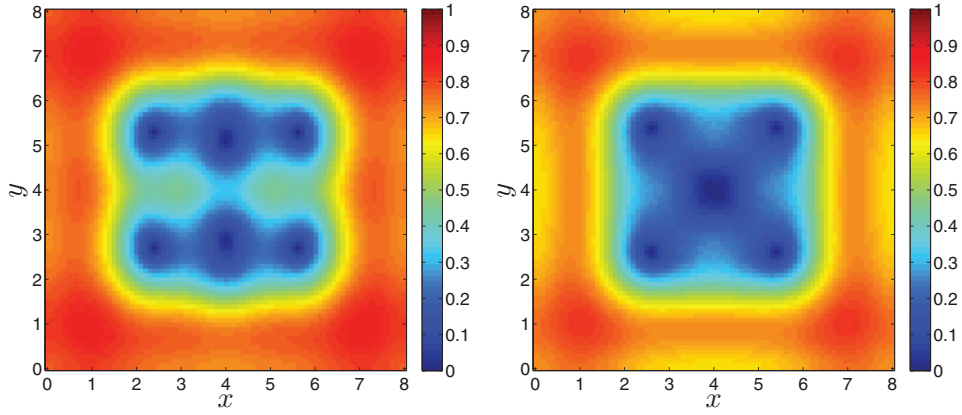

FIG. 6. Density plot of $|\psi_d|$ for six vortices at $H = 1.040$ (left) and $H = 1.125$ (right).

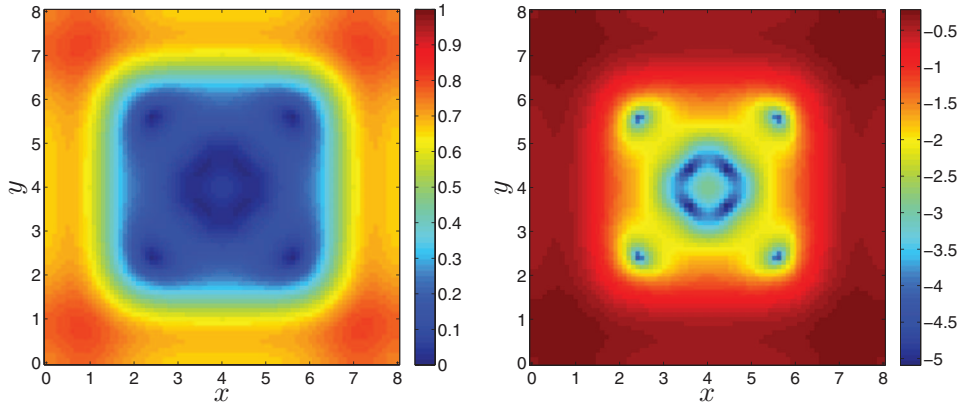

FIG. 7. The intensity plot of $|\psi_d|$ for eight vortices at $H = 1.260$ (left) and the same figure but using logarithmic scale (right).

This article is copyrighted as indicated in the article. Reuse of AIP content is subject to the terms at: http://scitation.aip.org/termsconditions. Downloaded to IP: 186.217.234.103 On: Fri, 10 Oct 2014 16:39:20

IX. CONCLUDING REMARKS

There are definitely many more important characteristics of a mesoscopic $(d + s)$-wave superconductor in comparison with the well-understood pure s-wave case. However, a detailed study of those properties will be postponed for a separate publication. In this paper, we restricted ourselves to developing a stable numerical algorithm to solve the TDGL equations which can be easily implemented and can be immediately applied in further simulations. We demonstrated the efficiency of our numerical procedure on a few peculiar examples of novel properties of mesoscopic mixed $(d + s)$-wave superconductors.

ACKNOWLEDGMENTS

We thank the Brazilian Agency FAPESP and Flemish Science Foundation (FSF) (FWO-Vlaanderen) for financial support. M.V.M. acknowledges support from the CAPES-PVE program.

[1] M. Tinkham, *Introduction to Superconductivity* (Krieger, Malabar, FL, 1975).
[2] Y. Ren, J. H. Xu, and C. S. Ting, Phys. Rev. Lett. **74**, 3680 (1995).
[3] J. H. Xu, Y. Ren, and C. S. Ting, Phys. Rev. B **53**, R2991 (1996).
[4] In Ref. 2, the authors write the two first terms of the free-energy functional density as $\alpha_s|\psi_s|^2 + \alpha_d|\psi_d|^2$ by considering α_s and α_{d0} as positive constants.
[5] A. Schmid, Phys. Kondens. Mater. **5**, 302 (1966).
[6] L. P. Gor'kov and G. M. Eliashberg, Zh. Eksp. Teor. Fiz. **54**, 612 (1968); Soviet Phys. - JETP **27**, 328 (1968).
[7] Q. Du, SIAM J. Appl. Math. **59**, 1225 (1999).
[8] P. I. Soininen, C. Kallin, and A. J. Berlinsky, Phys. Rev. B **50**, 13883 (1994).
[9] M. Franz, C. Kallin, P. I. Soininen, A. J. Berlinsky, and A. L. Fetter, Phys. Rev. B **53**, 5795 (1996).
[10] W. D. Gropp, H. G. Kaper, G. K. Leaf, D. M. Levine, M. Palumbo, and V. M. Vinokur, J. Comput. Phys. **123**, 254 (1996).
[11] H. G. Kaper and M. K. Kwong, J. Comput. Phys. **119**, 120 (1995).
[12] G. C. Buscaglia, C. Bolech, and A. López, in *Connectivity and Superconductivity*, edited by J. Berger and J. Rubinstein (Springer, Heidelberg, 2000).
[13] J. Berger, J. Math. Phys. **46**, 095106 (2005).
[14] E. Sardella, P. N. Lisboa-Filho, and A. L. Malvezzi, Phys. Rev. B **77**, 104508 (2008).
[15] P. DeGennes, *Superconductivity in Metals and Alloys* (Benjamin, New York, 1966).
[16] M. V. Milošević and R. Geurts, Physica C **470**, 791 (2010).
[17] M. M. Doria, J. E. Gubernatis, and D. Rainer, Phys. Rev. B **41**, 6335 (1990).
[18] Q. Du, M. D. Gunzburger, and J. S. Peterson, Phys. Rev. B **51**, 16194 (1995).
[19] B. J. Baelus and F. M. Peeters, Phys. Rev. B **65**, 104515 (2002).
[20] E. Sardella, A. L. Malvezzi, P. N. Lisboa-Filho, and W. A. Ortiz, Phys. Rev. B **74**, 014512 (2006).
[21] V. A. Schweigert, F. M. Peeters, and P. S. Deo, Phys. Rev. Lett. **81**, 2783 (1998); A. Kanda, B. J. Baelus, F. M. Peeters, K. Kadowaki, and Y. Ootuka, *ibid.* **93**, 257002 (2004); M. V. Milošević, A. Kanda, S. Hatsumi, F. M. Peeters, and Y. Ootuka, *ibid.* **103**, 217003 (2009); T. Cren, L. Serrier-Garcia, F. Debontridder, and D. Roditchev, *ibid.* **107**, 097202 (2011).
[22] J. J. Vicente Álvarez, G. C. Buscaglia, and C. Balseiro, Phys. Rev. B **54**, 16168 (1996).
[23] J. J. Vicente Álvarez, C. Balseiro, and G. C. Buscaglia, Phys. Rev. B **58**, 11181 (1998).
[24] V. F. Becerra, M. V. Milošević, F. M. Peeters, and E. Sardella, "Vortices and skyrmions in p-wave mesoscopic superconductors" (unpublished).
[25] The code is available on request.
[26] We know this from the phase of the order parameter which is shown in Figure 3. Following a closed loop near the boundary, the total phase difference is $\Delta = 2\pi L$, where L is the *vorticity*; the number of vortices if L is positive, and the number of anti-vortices if L is negative.
[27] We have drawn Figure 5 by separating Eq. (20) into two terms: $\mathbf{J}_s = \mathbf{J}_{sd} + \mathbf{J}_{ss}$, where $\mathbf{J}_{sd} = \mathrm{Re}\left(\bar{\psi}_d \mathbf{\Pi} \psi_d - \eta_v \bar{\psi}_s \Pi_x \psi_d \hat{x} + \eta_v \bar{\psi}_s \Pi_y \psi_d \hat{y}\right)$ and $\mathbf{J}_{ss} = \mathrm{Re}\left(\bar{\psi}_s \mathbf{\Pi} \psi_s - \eta_v \bar{\psi}_d \Pi_x \psi_s \hat{x} + \eta_v \bar{\psi}_d \Pi_y \psi_s \hat{y}\right)$.

This article is copyrighted as indicated in the article. Reuse of AIP content is subject to the terms at: http://scitation.aip.org/termsconditions. Downloaded to IP: 186.217.234.103 On: Fri, 10 Oct 2014 16:39:20